The Application of Depth Migration for Processing GPR Data

Dang Hoai Trung[1, *], *Nguyen* Van Giang[2], and *Nguyen* Thanh Van[1]

[1] Faculty of Physics and Engineering Physics, VNUHCM – University of Science

[2] Vietnam Academy of Science and Technology

Abstract. Migration methods play a significant role in processing ground penetrating radar data. Beside recovering the true image of subsurface structures from the prior designed velocity model and the raw GPR data, the migration algorithm could be an effective tool in bulding real environmental velocity model. In this paper, we have proposed one technique using energy diagram extracted from migrated data as a criterion of looking for the correct velocity. Split Step Fourier migration, a depth migration, is chosen for facing the challenge where the velocity varies laterally and vertically. Some results verified on field data on Vietnam show that migrated sections with calculated velocity from energy diagram have the best quality. **Key words** – Split Step Fourier, energy diagram, depth migration.

1 Introduction

Ground Penetrating Radar is the most accurate and fast method in surveying near-surface structures. There are five main steps for processing GPR data: removing bad data, filtering noise, gaining, calculating electromagnetic propagation velocity and migration. In seismic method, migration is usually the last step for collapsing diffraction hyperbolae on unmigrated sections to points, thus moving reflection events to their proper locations, creating a true image of subsurface structures [2, 7]. Nowadays, in GPR, migration can become a middle step of processing data for estimating true velocity.

There are two kinds of migration methods: time migration (using root mean square (RMS) velocity) and depth migration (using interval velocity). RMS velocity is the average velocity that are taken into account by considering the influence of the upper layer's instantaneous velocity; whereas the interval velocity only reflects the practical velocity of one layer. In our research, depth migration is chosen for producing highly detailed images.

2 Split Step Fourier Migration

Phase shift is a migration method considered vertically varying velocities and based on wavefield extrapolation [1]. Phase shift is performed in the frequency wave number domain, so a constant velocity must be used for each depth interval. To solve this problem, phase

* Corresponding author: dhtrung@hcmus.edu.vn

shift plus interpolation is introduced. In this method, image for each depth interval are extracted from migrations of different constant velocities and the results are combined to form last migrated section [5].

The SSF migration algorithm is an alternative to above methods. It is based on a modification to phase shift migration that makes it possible to accommodate lateral variations in the velocity for each migration interval. The lateral changes are considered as a perturbation; therefore, only one additional spatial Fourier transform is required for each depth extrapolation. We can split the laterally varying velocity field into a constant term and a small perturbation term [1, 4]:

$$v(x,z)=v_0(z)+\delta v(x,z) \tag{1}$$

Firstly, we use $v_0(z)$ to propagate wavefields in the (ω, k_z) domain [1]:

$$P^*=P(z,k_x,\omega)\exp\left[\pm i\sqrt{\left(\frac{\omega}{v_0(z)}\right)^2-k_x^2}\,\mathrm{d}z\right] \tag{2}$$

Then, P^* is transformed back to the (ω, x) domain, and a phase correction is applied to it to account for the lateral velocity variation [1]:

$$P(z+\mathrm{d}z,k_x,\omega)=\hat{P}^*\exp\left[\pm i\left(\frac{\omega}{v(x,z)}-\frac{\omega}{v_0(z)}\right)\mathrm{d}z\right] \tag{3}$$

The accuracy of SSF can be improved by making the propagator symmetric. That is, this term can be achieved by splitting the phase shift term into two identical parts and applying them before and after the wave propagation in the (ω, k_x) domain [1]:

$$\pm i\left(\frac{\omega}{v(x,z)}-\frac{\omega}{v_0(z)}\right)\mathrm{d}z=\pm i\left(2\cdot\frac{1}{2}\right)\left(\frac{\omega}{v(x,z)}-\frac{\omega}{v_0(z)}\right)\mathrm{d}z \tag{4}$$

However, for strong lateral variation of the velocity field, the perturbation theory fails, and more than one reference velocity must be used for SSF.

3 Field data

In this part, we illustrate the accuracy of SSF migration with some real data.

3.1 Underground Construction in Ho Chi Minh City street

The GPR data were collected by Detector Duo (IDS – Italy) with 700 MHz shielded antenna on a street of district 3, Ho Chi Minh City. In this GPR section after filtering noise (Fig. 1), we can see two hyperbole signals at 2.4 m and 5.4 m of distance. Note that black show negative values, while white is positive ones in Figure 2. The GPR machine emits the wavelet pulse with the strongest positive value in its early time. The reversed polarity of the reflection from the top of those two objects show high conductive anomalies. According to the prior information, this line crosses two subsurface metal water pipes.

The GPR section in figure 1 will be processed by finite-difference migration with the RMS velocity range of 0.06 to 0.15 m/ns (its jump valued 0.001 m/ns). We estimate a set of the total energy values extracted from migrated results with different velocities for one

specific zone. This zone is illustrated as a dashed rectangular in Figure 1. Each total energy value is summation of all energy points of migrated section from one velocity. Therefore, we can achieve a graph expressing relationship between total energy values and velocities [3]. Note that energy is square of amplitude.

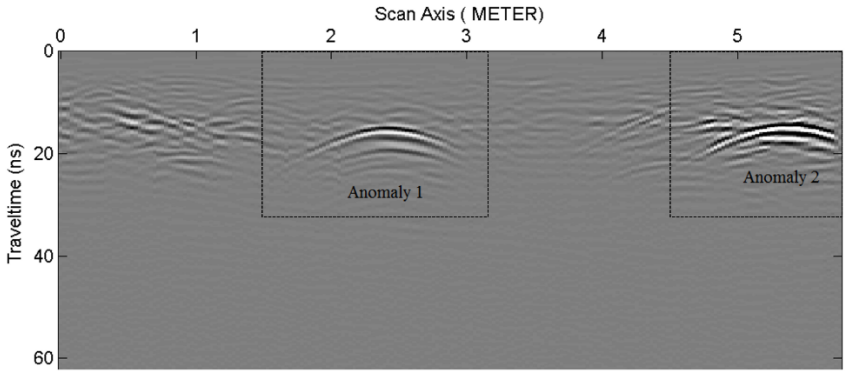

Fig. 1. GPR section after processing

The result shows that the calculating signal zone around the first hyperbole has maximum energy value at the velocity of 0.09 m/ns (Fig. 2a). Similarly, we also estimate the energy diagram of the second hyperbole. The results in Figure 3b show that the EM wave velocity in the environment above anomaly 2 is equal to 0.093 m/ns.

a) b)

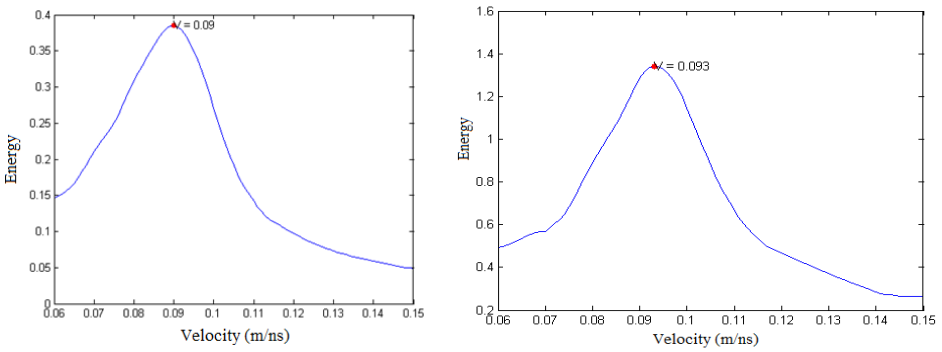

Fig. 2. Energy diagram of zone around: a) the first hyperbole; b) the second hyperbole

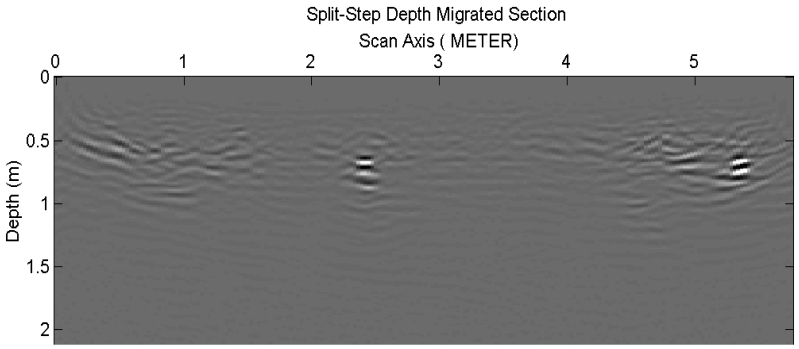

Fig. 3. The GPR migrated section by SSF

Generally, the use of maximum energy standard in order to optimize the migration problem has shown the variations in velocity laterally in this survey area. Therefore, SSF will be applied to migrate the GPR section (Fig. 3) [6]. On the migrated section, the two signals are clear and convergent. Consequently, the propagation velocities to the top of two hyperbolae are true. The depths and sizes of the two pipes based on the calculated velocity are d_1 = 0.65 m; Φ_1 = 142 mm and d_2 = 0.68 m; Φ_2 = 142 mm, respectively. This result has proven the accuracy of research method.

3.2 Surveying geology in Khanh Hoa province

The GPR data were collected by Zond 12e (Radar System – Latvia) with 150 MHz unshielded antenna at the seashore of Cam Lam district, Khanh Hoa province. The purpose of this survey is to determine the depth of a shell deposit layer. This is an organogenic structure that has been created from bay alluvial process. There are 5 longitudinal lines and 15 transverse lines at this survey area.

Based on data from two electrical resistivity imaging sections and a geological borehole, there three layers in the survey site:

– The first layer has rather low resistivity values which range from 120 to 160 Ωm. This layer can be interpreted as fine sand with its thickness of 3 m. It has been formatted from whitey grey, whitey yellow fine sand. It is in wet and loose state.
– The second layer has low resistivity values which range from 70 to 120 Ωm. This layer is also fine sand the same as the above layer, but it is in wet and medium dense to dense state.
– The last layer resistivity values are lower than 70 Ωm. This layer is muddy clay which consists of bluish grey, whitey grey, organic muddy clay. It is high plasticity and in water saturated and very soft state.

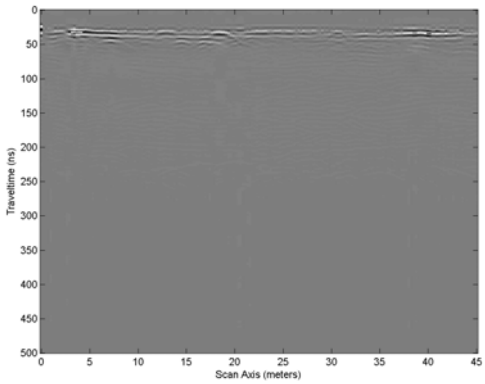

Fig. 4. The raw GPR section of line 5

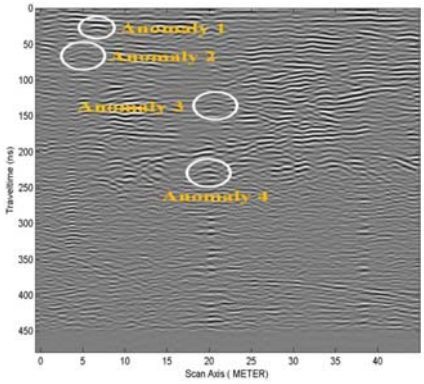

Fig. 5. The GPR section of line 5 after processing

We use the transverse line 5 and 14 to show the essential and accuracy of SSF migration. Figure 4 is a raw section of line 5 and Figure 5 is the section after processing. We can find a lot of hyperbolae in this image at x_1 = 14 m, t_1 = 22 ns; x_2 = 5.2 m, t_2 = 52 ns; x_3 = 20.6 m, t_3 = 126 ns and x_4 = 19.6 m, t_4 = 222 ns. Several hyperbolae at the depth of 200 to 250 ns can be reflection signals from the shell deposits. From 250 to 450 ns, the signal intensity decreases quickly due to low resistivity environment.

This GPR section will be processed by finite-difference migration with the RMS velocity range from 0.07 to 0.16 m/ns (its jump valued 0.001 m/ns) for signal zone around the first anomaly. The energy diagram (Fig. 6a) shows that the velocity at the apex of the hyperbola 1 (RMS velocity) is 0.141 m/ns (highest energy).

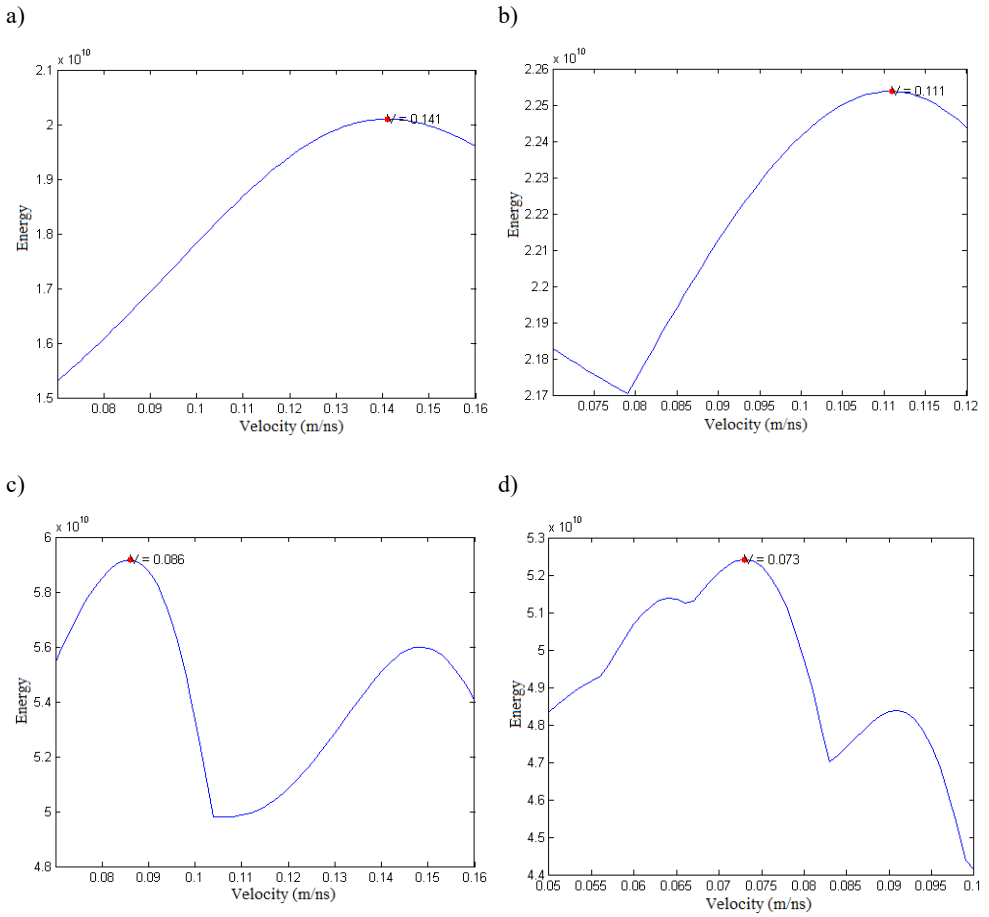

Fig. 6. The energy diagram of signal zone around the anomaly a) 1; b) 2; c) 3; d) 4

Similarly, the RMS velocity at the apex of the anomalies 2, 3 and 4 can be estimated at 0.111, 0.086 and 0.073 m/ns, respectively, from energy diagrams (Figs. 6b, c, d). To build the velocity model of this site, we must have the interval velocities derived from RMS velocities. The relevant formula of interval velocity and RMS velocity is shown as below [7]:

$$v_{\text{int}} = \sqrt{\frac{v_{rms2}^2 \tau_2 - v_{rms1}^2 \tau_1}{\tau_2 - \tau_1}} \tag{5}$$

We calculate the interval velocities by using the above equation and build the velocity model of this survey area as shown below (Fig. 7). We can see that the velocity varies strongly in vertical direction due to the change of water content of the coastline (according to geological borehole).

The SSF migrated section 5 using the above velocity model is shown in Figure 8. Evidently, all hyperbolae are convergent and the geological boundaries are clear and visible (see white arrows in Fig. 8). The time axis is changed to depth axis; thus, we can determine the depth of geological boundaries. The shell deposit layer can be recognized at the depth of 6–8 m (see white lines in Fig. 8).

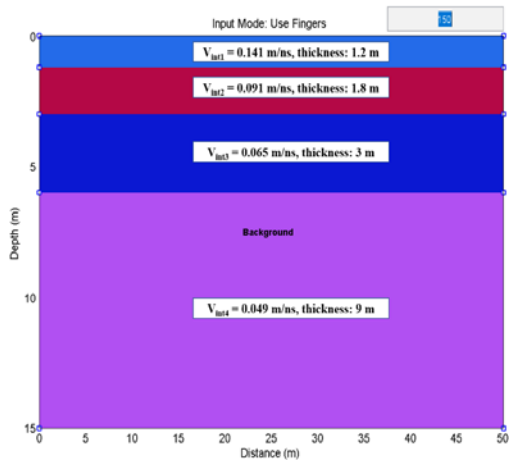

Fig. 7. The velocity model

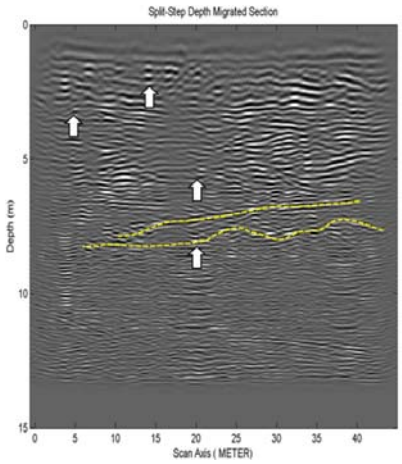

Fig. 8. The GPR migrated section 5

Similarly, we perform all above steps for line 14. The GPR sections before and after migration are shown in Figures 9a, b. We also recognize that all diffraction hyperbolae are collapsed, so the shell deposit boundary becomes easy to see (tracing positions of white arrows in Fig. 9b).

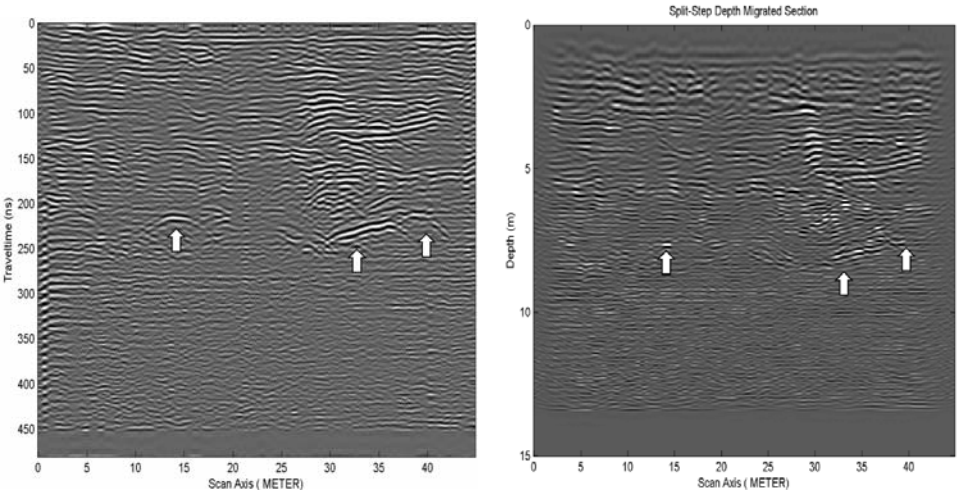

Fig. 9. The GPR section 14: a) before migration; b) after migration

4. Conclusion

We have presented the application of migration method to interpret GPR data and to build velocity model. Energy diagram is a good criterion to optimize the accuracy of determining propagation velocity by a migration algorithm. Split Step Fourier, depth migration, could solve the environment issue with velocity varying laterally and vertically. The migrated section is clear and reflect the depth of the apex of objects. Therefore, we can calculate exactly the size and the location of objects (example 1) and the depth of shell deposit layer (example 2) in migrated image.

However, the processing steps are complicated. Firstly, we must use time migration to calculate RMS velocity from energy diagram. Secondly, we need estimate the interval velocity from RMS velocity and build velocity model. Finally, SSF migration method is used to process GPR section. Therefore, this research should be expanded in the way of using depth migration to calculate energy diagram of each layer. The velocity that has highest energy can be an interval velocity of this layer. Thus, the processing steps become easier and decrease the error of determining interval velocity.

Acknowledgments

We would like to thank Cuong Van Anh Le from University of Science – VNUHCM Vietnam for his support.

References

1. B. Han, *A comparision of four depth migration methods*. SEG Technical Program Expanded Abstracts, pp. 1104–1107, doi:10.1190/1.1820080 (1998)
2. J. Gazdag and P. Sguazzero, *Migration of Seismic Data*. Proceedings of the IEEE, 72(10), pp. 1302–1315 (1984)
3. V.T. Nguyen, V.A.C. Le, T.V. Nguyen, H.T. Dang, M.T. Vo and N.N.L. Vo, *Energy Analysis in Semiautomatic and Automatic Velocity Estimation for Ground Penetrating Radar Data in Urban Areas: Case Study in Ho Chi Minh City, Vietnam*. Advances and Applications in Geospatial Technology and Earth Resources, Springer International Publishing, ISBN: 978-3-319-68239-6 (2017)
4. A.R. Sena, P.L. Stoffa and M.K. Sen, *Split-step Fourier migration of GPR data in lossy media*. Geophysics, Vol 71 (4), pp. 77–91, doi: 10.1190/1.2217157 (2006)
5. P.L. Stoffa, J.T. Fokkema, R.M.D.L. Freire and W.P. Kessinger, *Split-Step Fourier Migration*. Geophysics, Vol 55, No. 4, pp. 410–421, doi: 10.1190/1.1442850 (1990)
6. A.Tzanis, 2006. MATGPR: *A freeware MATLAB package for the analysis of common-offset GPR data*. Geophysical Research Abstracts, Vol. 8, 09488, 2006
7. O. Yilmaz, *Seismic Data Analysis, Chapter 4*. Society of Exploration Geophysicist, Electronic Edition, ISBN 978-0-931830-46-4, pp. 476–491 (1987)